Submitted, accepted and published by
Energy & Fuels, 2010, 24, 1402-1413

Ilmenite Activation during Consecutive Redox Cycles in Chemical-Looping Combustion

Juan Adánez[*]*, Ana Cuadrat, Alberto Abad, Pilar Gayán, Luis F. de Diego, and Francisco García-Labiano*

Department of Energy and Environment, Instituto de Carboquímica (CSIC), Miguel Luesma Castán 4, 50018 Zaragoza, Spain

RECEIVED DATE (to be automatically inserted after your manuscript is accepted if required according to the journal that you are submitting your paper to)

[*] Corresponding author: Tel.: +34 976 733977. Fax: +34 976 733318. E-mail: jadanez@icb.csic.es

ABSTRACT. Ilmenite, a natural mineral composed of $FeTiO_3$, is a low cost and promising oxygen carrier, OC, for the solid fuels combustion in a Chemical-Looping Combustion (CLC) system. The aim of this study is to analyze the behavior of ilmenite as OC in CLC and the changes in its properties through redox cycles. Experiments consisting of reduction-oxidation cycles in a thermogravimetric analyzer were carried out using the main products of coal pyrolysis and gasification, that is, CH_4, H_2 and CO, as reducing gases. Characterizations of ilmenite through SEM-EDX, XRD, Hg porosimetry, N_2 fisisorption, He pycnometry and hardness measures have been done. Both fresh and previously calcined at 1223 K ilmenite have been used as initial OCs. Fresh ilmenite reacts slowly; nevertheless there is a gain in reactivity in reduction as well as in oxidation with the number of cycles. This activation occurs for all tested fuel gases and is faster if ilmenite has been previously calcined. The initial oxygen

transport capacity was measured to be 4% and it decreases with the number of cycles up to 2.1% after 100 redox cycles. Nevertheless, ilmenite shows adequate values of reactivity and oxygen transport capacity for its use in the CLC technology with solid fuels. The trade-off between the increase in reactivity and the decrease in oxygen transport capacity on ilmenite performance in a CLC system has been evaluated through the estimation of the solids inventory needed in the fuel reactor. If fresh or calcined ilmenite is fed into the CLC system, the activation process could happen in the CLC itself. Also a previous step for activation can be designed.

INTRODUCTION

At present there is a general consensus on the need of reducing the emissions of the greenhouse gas CO_2 in order to restrain climate change. Anthropogenic CO_2 is mainly generated in combustion of fossil fuels, which are foreseen to provide about 80% of the overall world consumption of energy for the next several decades. When regarding the energy-related CO_2 emissions by fuel type, coal use generated 39% of the emissions in 2004 and it is estimated that the percentage in 2030 will rise up to 43%.[1,2] Among the different opportunities to reduce the anthropogenic CO_2 emissions, carbon capture and sequestration (CCS) has been identified as a relevant option for in stationary power plants using fossil fuels. In this context, Chemical-Looping Combustion (CLC) is one of the most promising technologies to carry out CO_2 capture at a low cost.[3-5]

CLC is based on the transfer of the oxygen from air to the fuel by means of a solid oxygen carrier that circulates between two interconnected fluidized beds, avoiding direct contact between fuel and air.[6] Important progress has been made in CLC for gaseous fuels (natural gas and syngas) to date. Several authors have successfully demonstrated the feasibility of this process in different CLC prototypes in the 10-140 kW_{th} range using oxygen carriers based on nickel and cobalt oxides,[7] NiO,[8-11] and CuO.[12] Also, there is an increasing interest for the application of CLC using coal, regarding the intensive use of this fuel for energy generation. There are two possibilities for the use of the CLC technology with coal. The first one is to carry out previous coal gasification and subsequently to introduce the produced gas in the CLC system. Simulations performed by Jin and Ishida[13] and Wolf et al.[14] showed that this process has

the potential to achieve an efficiency of about 5-10% points higher than a similar combined cycle with conventional CO_2 capture technology. Several oxygen carriers based on Ni, Cu, Fe and Mn oxides have shown good reactivity with syngas components, i.e. H_2 and CO,[15,16] and the use of syngas in a CLC system has been successfully accomplished in 300-500 W_{th} continuous CLC units.[17-21]

The second possibility for the use of coal in CLC is the direct combustion in the CLC process, that is, avoiding the need of coal gasification and the corresponding gaseous oxygen requirement.[22-23] The reactor scheme for this CLC configuration is shown in Figure 1. In this option coal is physically mixed with the oxygen carrier in the fuel reactor and the carrier reacts with the gas products from steam coal gasification, where H_2 and CO are main components. Thus, the solid fuel gasification proceeds in the fuel reactor first according to reactions (1-3) and the resulting gases and volatiles are oxidized through reduction of the oxidized oxygen carrier, Me_xO_y, by means of reaction (4). The oxygen carrier reduced in the fuel reactor, Me_xO_{y-1}, is transferred to the air reactor where reaction (5) with oxygen from air takes place. Thus the oxygen carrier is regenerated to start a new cycle. The net chemical reaction is the same as usual combustion with the same combustion enthalpy.

$$\text{Coal} \rightarrow \text{Volatile matter} + \text{Char} \quad (1)$$

$$\text{Char} + H_2O \rightarrow H_2 + CO \quad (2)$$

$$\text{Char} + CO_2 \rightarrow 2\ CO \quad (3)$$

$$H_2, CO, \text{Volatile matter } (CH_4) + n\ Me_xO_y \rightarrow CO_2 + H_2O + n\ Me_xO_{y-1} \quad (4)$$

$$Me_xO_{y-1} + \tfrac{1}{2}\ O_2 \rightarrow Me_xO_y \quad (5)$$

Ideally, the stream of combustion gases from the fuel reactor contains primarily CO_2 and H_2O, although some unburnt compounds can also appear (CO, H_2, CH_4, volatiles). In this case, an oxygen polishing step can be necessary for complete combustion to CO_2 and H_2O. After that, water can be easily separated by condensation and a highly concentrated stream of CO_2 ready for compression and sequestration is achieved. The CO_2 capture is inherent to this process, as the air does not get mixed with the fuel, and no additional costs or energy penalties for gas separation are required. The gas stream from the air reactor is oxygen-depleted and consists in N_2 and some unreacted O_2.

It is expected that the gasification process was the limiting step in the fuel reactor, so the stream of solids exiting from the fuel reactor could contain some unconverted char together with the oxygen carrier. Thus, for solid fuels an additional carbon stripper it is necessary to separate char particles from oxygen carrier particles and so reducing the amount of carbon transferred from the fuel reactor to the air reactor. It is necessary to point out that the transference of char to the air reactor does not reduces the energetic efficiency of the process but it decreases the carbon capture efficiency of the system because some CO_2 will exit together with the exhaust gas from the air reactor. Moreover, as a consequence of the ash present in the solid fuel it is necessary to drain ashes from the system to avoid its accumulation in the reactors. The drain stream will also contain some amount of oxygen carrier. Thus, it is expected that the active life of this material would be limited by the losses together the drain stream rather than for its degradation. The efficiency of char combustion in the fuel reactor and the separation of ash from the oxygen carrier seem to be key factors for the development of this process.

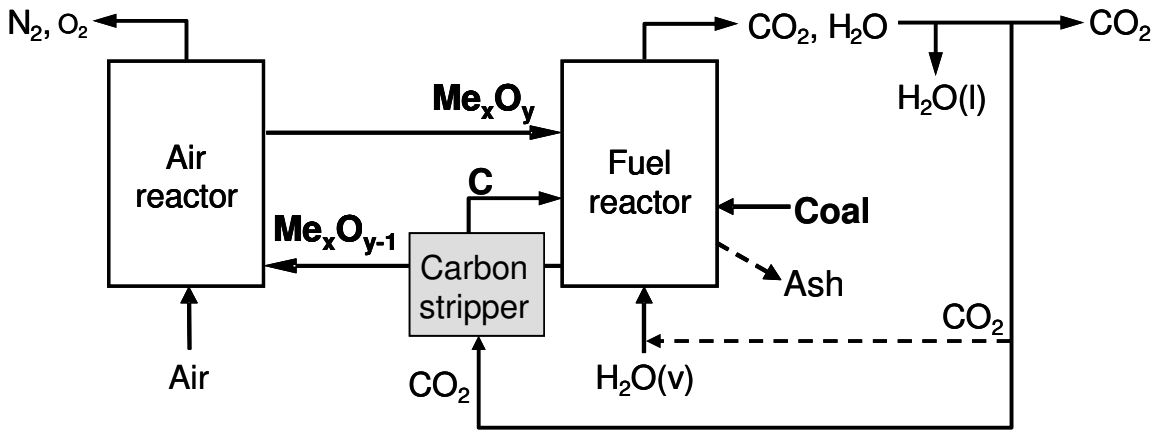

Figure 1. Reactor scheme of the CLC process using solid fuels. (– – – - optional stream)

As for gaseous fuels, suitable oxygen carriers for solid fuels in the CLC process must have high selectivity towards CO_2 and H_2O, enough oxygen transport capacity, high reactivity, high mechanical strength, attrition resistance and agglomeration absence. All these characteristics must be maintained during many reduction and oxidation cycles. There are studies made on the reactivity of synthetic oxygen carriers based on CuO,[24] Fe_2O_3[25-26] and NiO[27] for in-situ gasification of the solid fuel. However,

low cost of the carrier is rather desirable for its use with coal, as it is predictable a partial loss together with the coal ashes when removing them from the reactor to avoid their accumulation in the system. The use of natural minerals for this option seems to be very interesting, ilmenite being an appropriate material.[28] Ilmenite is mainly composed of $FeTiO_3$ ($FeO \cdot TiO_2$), where iron oxide is the active phase that behaves as an oxygen carrier. There are a few recent studies showing an acceptable performance of ilmenite as an oxygen carrier in CLC at different scales. Leion et al.[28,29] analyzed the reactivity of ilmenite in a batch fluidized bed for solid fuels combustion. Ilmenite gave high conversion of CO and H_2 but moderate conversion of CH_4. They observed a gain in ilmenite reactivity as increasing redox cycles, and eventually reactivity as high as for a synthetic Fe_2O_3-based oxygen carrier was reached. Berguerand et al.[30,31] operated a 10 kW_{th} chemical-looping combustor using South African coal and petroleum coke as solid fuels. They concluded that ilmenite appeared to be a suitable material to be used for solid fuel combustion in a CLC system. The encouraging results obtained to date indicate that there is still further research to be carried out.

The aim of this work is to study the performance and activation of ilmenite as oxygen carrier in a CLC system with the main gases from coal gasification, that is, H_2, CO and CH_4. To do this, consecutive reduction-oxidation cycles were carried out in a thermogravimetric analyzer (TGA) and to analyze the activation process a characterization of the initial and reacted samples of the oxygen carrier was done.

EXPERIMENTAL SECTION

The behavior of ilmenite as oxygen carrier to be used in a CLC system has been analyzed by consecutive redox cycles in a thermogravimetric analyzer (TGA) system.

Oxygen carrier. Ilmenite is a common mineral found in metamorphic and igneous rocks mainly composed by $FeTiO_3$. In principle, when using ilmenite as oxygen carrier in a CLC process, the reduced form consists in $FeTiO_3$ ($FeO + TiO_2$) and the most oxidized level is Fe_2TiO_5, which corresponds to $Fe_2O_3 + TiO_2$. The ilmenite used in this study is a concentrate from a natural ore. Fresh ilmenite and

ilmenite particles after a thermal treatment were used in this work. The calcination of fresh ilmenite was made at 1223 K in air during 24 hours. The calcination was considered in order to improve properties and initial reaction rates,[32] and to get ilmenite in its most oxidized state, as it has been already done by Leion.[29] Moreover, a pre-oxidation of ilmenite was also beneficial in order to avoid defluidization problems.[33]

Ilmenite particles were physically and chemically characterized by several techniques. The real density of the particles was measured with a Micromeritics AccuPyc II 1340 Helium picnometer. The force needed to fracture a particle was determined using a Shimpo FGN-5X crushing strength apparatus. The mechanical strength was taken as the average value of at least 15 measurements undertaken on different particles of each sample randomly chosen. Particle porosity was measured by Hg intrusion in a Quantachrome PoreMaster 33. The identification of crystalline chemical species was carried out by powder X-ray diffraction (XRD) patterns acquired in an X-ray diffractometer Bruker AXS D8ADVANCE using Ni-filtered Cu Ka radiation equipped with a graphite monochromator.

Thermogravimetric analysis. The effect of consecutive reduction-oxidation cycles on the reactivity of fresh and precalcined ilmenite using various reducing gas compositions was tested in a thermogravimetric analyzer (TGA), CI Electronics type. A detailed description of the apparatus and procedure can be found elsewhere.[34]

For the experiments, about 50 mg of ilmenite particles was loaded on the platinum basket. The system was heated to 1173 K in N_2 atmosphere. After reaching the set temperature, the experiment was started by exposing the oxygen carrier to alternating reducing and oxidizing conditions. To prevent reducing gas and air as oxidizing agent from mixing, a nitrogen flow was passed for two minutes after the oxidizing and reducing processes. The composition of the gas during reduction period was 15% H_2 + 20% H_2O, 15% CO + 20% CO_2 or 15% CH_4 + 20% H_2O, depending on the reducing gas used, and N_2 to balance. The addition of steam to the reducing gas flow was made by bubbling the gas flow through a saturator containing water at the temperature of saturation at the desired steam concentration. Subsequent oxidation was carried out by air.

RESULTS AND DISCUSSION

Characterization of ilmenite particles. Table 1 shows the main properties for fresh and calcined ilmenite. The fresh ilmenite used in this study was the same one used by Leion et al.[28] and has a purity of 94.3%. The inert part is a mixture of oxides containing $MgSiO_3$ as main compound. Through SEM analysis it could be observed that the inert part is clearly distinguishable as a separated phase from the active part formed by iron and titanium compounds. The XRD analysis revealed ilmenite ($FeTiO_3$), hematite (Fe_2O_3) and rutile (TiO_2) as major components of fresh ilmenite. Besides, SEM-EDX analyses revealed a Fe:Ti molar relation around 1:1.

Calcined ilmenite consists of a mixture of ferric pseudobrookite (Fe_2TiO_5), rutile (TiO_2) and some free hematite (Fe_2O_3), which confirms the literature data indicating that iron compounds in ilmenite are in the most oxidized state after calcination at 1223 K.[32,35] To analyze the effect of the calcination time, samples were calcined during 1, 2, 6 and 24 hours. For 2, 6 and 24 hours the same XRD profiles are obtained, so it would be necessary that the pre-treatment lasted only 2 hours.

Table 1. Characterization of fresh, calcined and activated ilmenite

	Fresh	**Calcined**	**Activated**
XRD (main species)	$FeTiO_3$, Fe_2O_3, TiO_2	Fe_2TiO_5, Fe_2O_3, TiO_2	Fe_2TiO_5, Fe_2O_3, Fe_3O_4, TiO_2
True density (kg/m^3)	4580	4100	4250
Porosity (%)	0	1.2	35
Particle diameter (μm)	150-300	150-300	n.a.
BET Surface (m^2/g)	0.6	0.8	0.4
Crushing strength (N)	2.4	2.2	1.0

Mercury porosimetry of both fresh and calcined ilmenite exhibit low porosity development. Low values of BET surface area were measured, but a slight increase was observed after calcination. The values of crushing strength obtained are similar to other Fe-based oxygen carriers and they are

acceptable for the use of these particles in circulating fluidized bed.[36] Table 1 also includes the main properties of activated particles after several redox cycles, and they will be discussed later.

Table 2. Mass variations of ilmenite when reduced to various oxidation states at 1173 K and iron containing species determined by XRD.

H_2O/H_2	Mass loss	Final state of reduced Fe_2O_3	Final state of reduced Fe_2TiO_5
50	4.0 %	Fe_3O_4	$FeTiO_3$, Fe_2TiO_4
1.34	4.8 %	FeO	$FeTiO_3$, Fe_2TiO_4

Table 3. Calculated ilmenite composition (wt.%)

	Fresh ilmenite	Calcined ilmenite
Fe_2O_3	14.8	11.2
$FeTiO_3$	65.5	-
Fe_2TiO_5	-	54.7
TiO_2	14.0	28.6
inerts	5.7	5.5

Ilmenite composition was calculated through weight variations during oxidation or reduction of fresh ilmenite. Fresh ilmenite is mainly composed by $FeTiO_3$, Fe_2O_3 and TiO_2. When ilmenite is calcined, a gain of 3.5 wt.% is observed due to the oxidation of $FeTiO_3$ (Fe^{2+}) to Fe_2TiO_5 (Fe^{3+}). This means that the fraction of $FeTiO_3$ in the raw material should be 65.5% considering the stoichiometric oxidation of Fe^{2+} to Fe^{3+}. In addition, Table 2 shows the results from experiments carried out with calcined ilmenite in thermobalance at 1173 K and varying the H_2O/H_2 ratio. Depending on the H_2O/H_2, ratio, the reduction of free Fe_2O_3 can finish in Fe_3O_4, FeO or Fe because of thermodynamic equilibrium.[16] At 1173 K, for $H_2O/H_2 < 0.6$ free Fe_2O_3 can be reduced to metallic Fe^0, whereas for $H_2O/H_2 > 2.7$ the reaction proceeds only until the formation of Fe_3O_4.[16] At H_2O/H_2 ratios between these values, free Fe_2O_3

is reduced to FeO. However, in all cases Fe_2TiO_5 is reduced to $FeTiO_3$ or Fe_2TiO_4, corresponding to Fe^{2+}.[28] Consequently, the mass loss observed in each case should be different depending on the final oxidation state of Fe from reduction of free Fe_2O_3. Considering these mass variations, the resulting ilmenite composition is shown in Table 3. The Fe:Ti molar ratio so obtained was 1:1.

Ilmenite reactivity. Several reduction-oxidation cycles were carried out in TGA to analyze the reactivity of fresh and activated ilmenite. Oxidizing as well as reducing times for each cycle were set to 30 minutes. Figure 2 represents the sample mass variation during 10 cycles for fresh ilmenite. A mass value of 100% is assumed to be the sample in its most oxidized state. The initial mass is 3.5% lower, i.e. 96.5%, corresponding to the composition of fresh ilmenite. At the beginning, it can be observed that ilmenite is not completely reduced or oxidized after the fixed reacting time. However, there is an increase in both the reduction and oxidation extension during the repeated redox cycles. The mass loss is considered to be exclusively due to oxygen transfer and it is stabilized at a value of 4.8% after 4 cycles, which is the maximum mass loss expected from the ilmenite composition estimation, see Table 2. Therefore, it was observed an activation process which made that the reactivity increased during the first redox cycles.

Figures 3 and 4 show the normalized conversion for the reduction, $X_{N,r}$, and the oxidation, $X_{N,o}$, reactions with time for consecutive cycles of fresh ilmenite calculated from the mass variations registered in TGA as

$$X_{N,r} = \frac{m_o - m}{m_o - m_r} = \frac{m_o - m}{R_o m_o} \tag{6}$$

$$X_{N,o} = 1 - X_{N,r} = \frac{m - m_r}{R_o m_o} \tag{7}$$

where m is the instantaneous mass, and m_o and m_r are the mass of fully oxidized and reduced ilmenite at the reacting condition, respectively. The oxygen transport capacity, R_o, was defined as the mass fraction of the oxygen carrier that is used in the oxygen transfer, calculated as

$$R_o = \frac{m_o - m_r}{m_o} \tag{8}$$

For the calculation of the normalized conversion a value of R_o = 4.8% was considered in all cases.

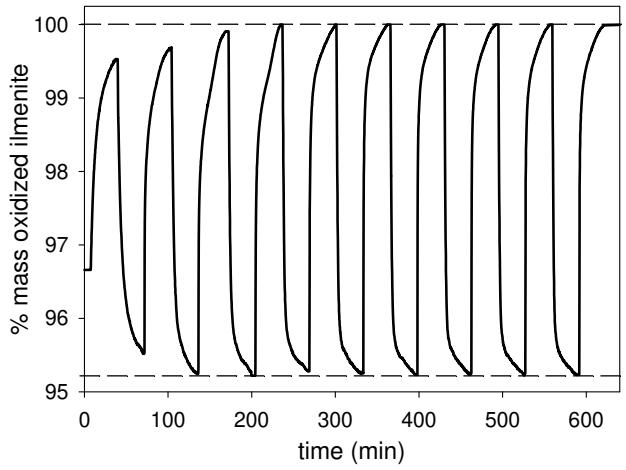

Figure 2. Mass variations during reduction-oxidation cycles in TGA starting from fresh ilmenite. Reduction and oxidation times: 30 minutes. Reducing gas: 15% CH_4 + 20% H_2O. Oxidation by air. T = 1173 K.

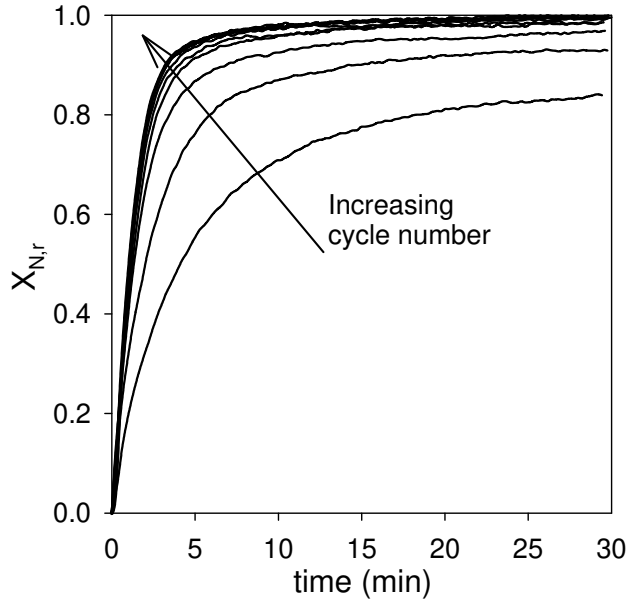

Figure 3. Normalized conversion during reduction period of fresh ilmenite vs. time through several cycles. Reducing gas: 15% CH_4 + 20% H_2O. Nitrogen to balance. T = 1173 K.

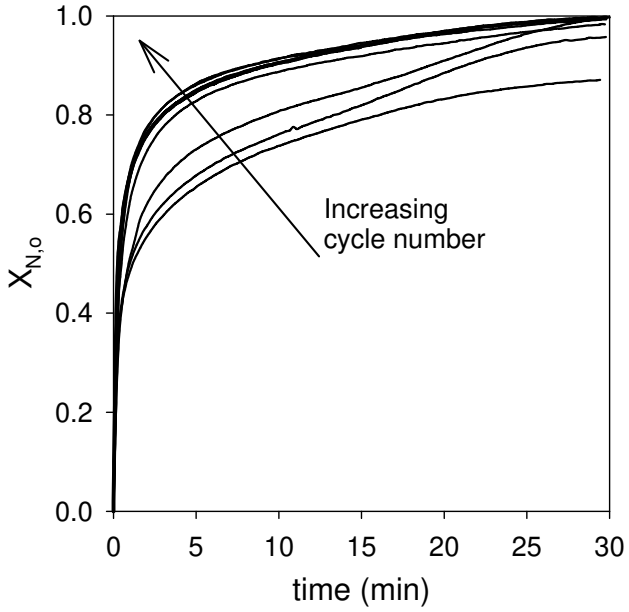

Figure 4. Normalized conversion during oxidation period in air of fresh ilmenite vs. time through several cycles. Nitrogen to balance. T = 1173 K.

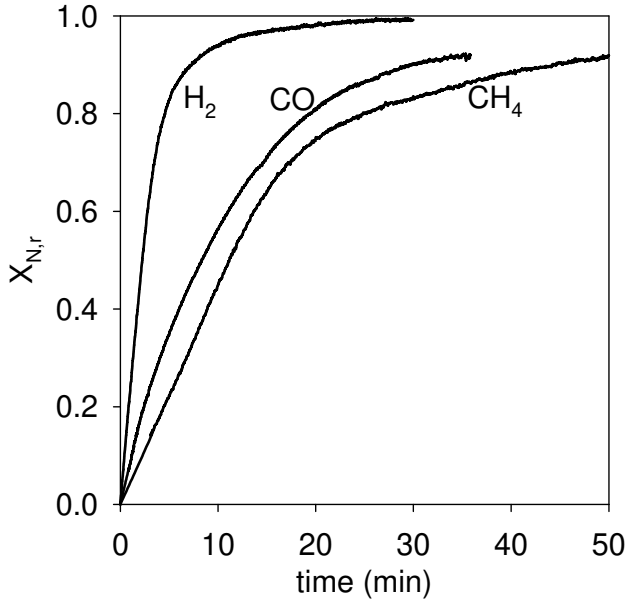

Figure 5. Normalized conversion during reduction period of calcined ilmenite vs. time for different reducing gases: 15% H_2 + 20% H_2O, 15% CO + 20% CO_2 and 15% CH_4 + 20% H_2O. Nitrogen to balance. T = 1173 K.

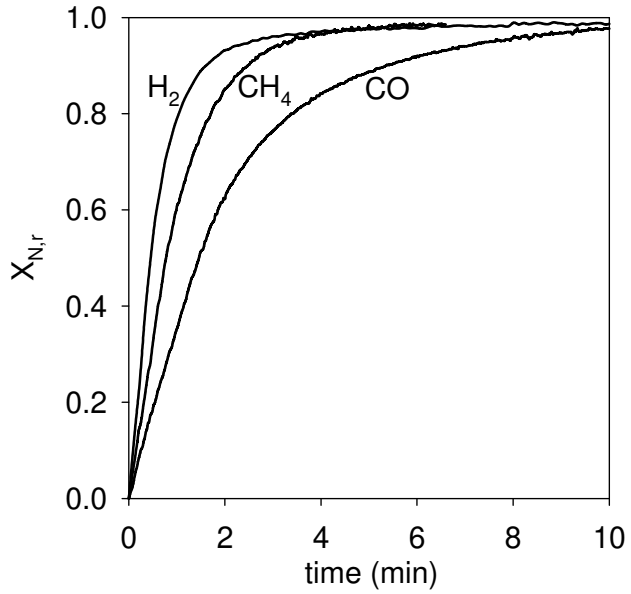

Figure 6. Normalized conversion during reduction period of activated ilmenite vs. time for different reducing gases: 15% H_2 + 20% H_2O, 15% CO + 20% CO_2 and 15% CH_4 + 20% H_2O. Nitrogen to balance. T = 1173 K.

Although ilmenite presents initially a rather low reactivity, the oxygen carrier has a gradual gain in its reduction reaction rate as well as in oxidation rate. The reactivity increases up to a maximum value after several cycles and stabilizes. This increase is more pronounced in the reduction reaction than in the oxidation reaction, because the initial reactivity for the oxidation of ilmenite for the first oxidation step is relatively high, with $X_{N,o}$ = 0.25 in less than 9 seconds for fresh ilmenite. After 4 cycles carried out in TGA a value for the normalized conversion of 0.8 is reached in 120 s for reduction and 180 s for oxidation reaction. At this point, it can be considered that ilmenite had achieved maximum conversion rate in both reduction and oxidation reactions. Also, it can be observed that the oxidation rate decreases gradually at high conversion values ($X_{N,o}$>0.8), reaching full conversion in 30 minutes. This fact indicates that a change in the resistance control has happen or the oxidation reaction proceeds via two consecutive steps.

Similar behavior was observed for redox cycles using H_2 and CO as reducing gases. For the different reducing gases, fresh, calcined and activated ilmenite react faster with H_2 than with CO and CH_4. Figures 5 and 6 show the conversion vs. time curves for the different reducing gases for calcined and

activated ilmenite, respectively. Observe that the time scales are different in these Figures. Calcined ilmenite reacts faster with CO than with CH_4, unlike activated ilmenite. For H_2 and CO the reactivity increases around 5 times after the activation, while for CH_4 this increase is about 15 times. The reactivity increase observed for all these fuel gases can be explained through the structural changes undergoing the solid during consecutives redox cycles, which will be discussed later.

Effect of precalcination on ilmenite activation. Samples of fresh and calcined ilmenite were subjected to alternating reduction-oxidation cycles using CH_4, H_2 or CO as reducing gases. Hundred cycles were performed and the reducing and oxidizing periods were one minute. Thus, the effect of the extension of reduction can be also analyzed comparing the results to that showed in Figure 2. Figure 7 represents the final normalized conversion, $X_{N,r}$, reached after each reducing period using CH_4 as reducing gas. Both samples showed an increase in the $X_{N,r}$ reached with the cycles up to a constant value. This was related to the fact that the reaction rate was higher in each cycle during the activation period before stabilizing. After that, no gain in the reaction rate was observed.

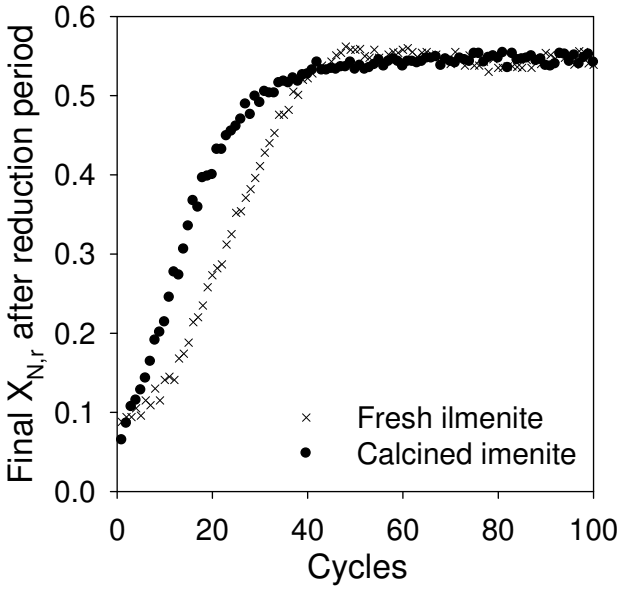

Figure 7. Comparison of the evolution of the final normalized conversion reached after the reduction period of fresh and calcined ilmenite through several cycles. Reduction and oxidation time: 1 minute. Reducing gas: 15% CH_4 + 20% H_2O. Nitrogen to balance. T = 1173 K.

Both fresh and calcined ilmenite achieve the same conversion level after activation, but it can be however observed that calcined ilmenite reached earlier the activated state. Whereas 40 cycles were necessary for the activation and stabilization for fresh ilmenite, about 30 cycles were enough to activate calcined ilmenite. Therefore, a previous calcination has a positive effect on both the reactivity of the oxygen carrier and the activation rate during the activation period. Similar behavior was found when the activation was carried out using 15 vol.% H_2 or 15 vol.% CO as reducing gases, but in these cases calcined ilmenite activates in 9 cycles with H_2 and in 20 cycles with CO.

Effect of the extension of reduction on ilmenite activation. Experimental results where the reducing and oxidizing periods were 30 min and 1 min are showed in Figures 2 and 7, respectively. The activation took only 4 cycles when the reacting periods were 30 min, whereas about 30-40 cycles were necessary when the reacting periods were 1 min. Thus, the activation state was clearly reached in a lower number of redox cycles when the redox periods were 30 min than when the redox periods were 1 min. This fact was because the reduction conversion reached in each cycle was higher as the reducing period was longer. The reduction conversion for 30 min was higher than 90%, but the conversion for 1 min was in the range 10-50%. Leion et al.[28] also observed the activation of ilmenite during about 20 cycles before stabilizing, when the conversion reached in each cycle was around 50%. Therefore, the reduction conversion reached in each cycle has an important effect on the number of cycles needed to activate the ilmenite: the higher is the reduction conversion the less number of cycles are needed to activate ilmenite. Nevertheless, the total time used during reducing periods for activation of fresh ilmenite was 40 min for reducing periods of 1 min and 120 min for reducing periods of 30 min.

The activation period showed for the different reducing gases also can be explained for the diverse conversion reached in every redox cycle. The reactivity initially followed the order $H_2 > CO > CH_4$, see Figure 5. Therefore the conversion reached during the reduction period –1 min in all cases– followed the same order, which explains that the number of redox cycles necessary for the ilmenite activation was in the reverse order $CH_4 > CO > H_2$.

The activation process has a beneficial and strong influence on the reactivity in both the oxidation and reduction reactions. To accelerate the activation process, calcined ilmenite should be preferred to fresh ilmenite. The activation of ilmenite particles is a process that can happen in the CLC system itself. Thus, the activation process should be considered during the startup period. At steady state, most of particles in the CLC system should be activated ilmenite. Only a small fraction could be non-activated particles, corresponding to the makeup flow to flow to maintain the solids holdup in the fuel reactor. Thus, the feeding of non-activated particles in the CLC system should not have a big effect on the CLC performance. In this case, the activation rate will depend on the operating conditions, e.g. the residence time in the fuel reactor which affect to the extension of reduction.

Nevertheless, in view of the relatively fast activation process, it could be advantageous for starting the operation to activate ilmenite particles previously to introduce them to the CLC system. Moreover, it can be beneficial for the economy of the process to carry out the activation in multiple short cycles instead of few long cycles because lower time is spent.

Structural changes during activation. In order to explain the activation observed by ilmenite during the calcination and during redox cycles, a morphological characterization of each sample was done by SEM. Figure 8 shows SEM microphotographs that confirm the lack of pores in fresh ilmenite and a slight gain in porosity after calcination. Throughout the reduction-oxidation cycles, there is continuous appearance of macropores or cracks, which generate a rise in porosity up to values of 35% for completely activated ilmenite. In Figure 8 can be observed a quite sharp-edged surface in fresh ilmenite, and the active phase surface begins to conform to a granular shape after calcination. The granulation is enhanced during redox cycles, as can be observed for activated ilmenite. This appearance of grains leads to a higher reaction surface, and likely this fact would be the reason for the reactivity increase with the cycle number. Similar results are found in the literature when natural minerals based on iron are used as oxygen carriers. Mattisson et al.[37] found the reactivity of an iron ore increased with redox cycles, likely due to the development of cracks and fissures in the particle. According to the work by Leion et al.[28], the porosity development is also important for ilmenite with redox cycles.

Figure 9 shows the SEM image of a particle activated after repeated redox cycles. An external shell slightly separated from the rest of the particle was observed. The space between the shell and the core also enhances the porosity measured for the particle. This shell is gradually generated and grows with the number of cycles. EDX analyses were done to determine Fe and Ti distributions throughout the particles, see Figure 10. In fresh and calcined ilmenite distributions of both elements were uniform, which agrees with the XRD analysis that reveals Fe_2TiO_5 as main component. For activated ilmenite the particle core is titanium enriched, whereas the external part is iron enriched. XRD analyses to the external part found that this region is composed only by iron oxide, whereas XRD to the internal core revealed the existence of TiO_2 and Fe_2TiO_5. Thus, the external shell formed during activation period was Fe enriched, likely due to a migration phenomenon of iron oxide towards the external part of the particle, where there is not TiO_2 to form iron titanates. The segregation of Fe_2O_3 from the titanium-rich phase also has been reported in the literature because of the migration of Fe^{2+} or Fe^{3+} ions through the solid lattice towards the grain boundary during the oxidation step.[38,39]

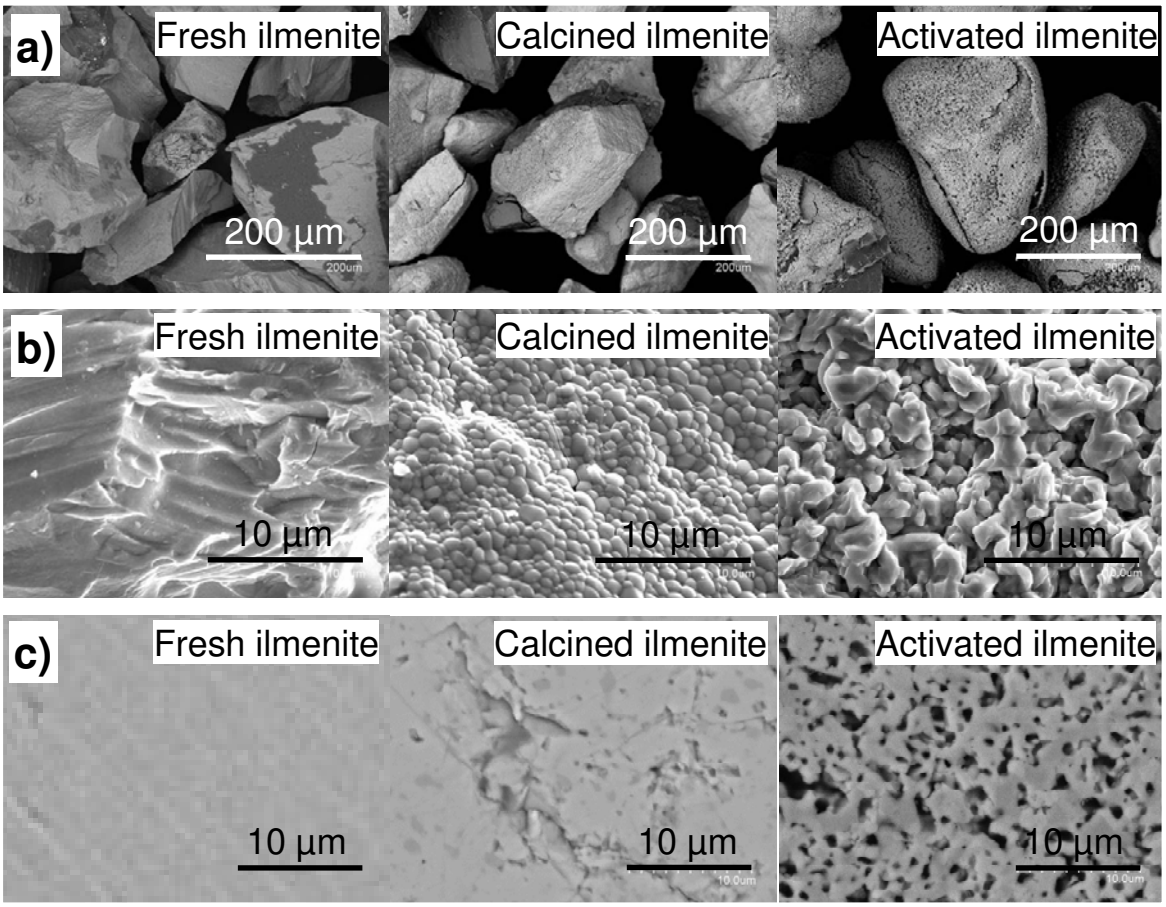

Figure 8: SEM images of (a) a general overview of several particles, (b) the external surface of the particles, and (c) a detail of the cross section inside the particles for the fresh, calcined and activated ilmenite.

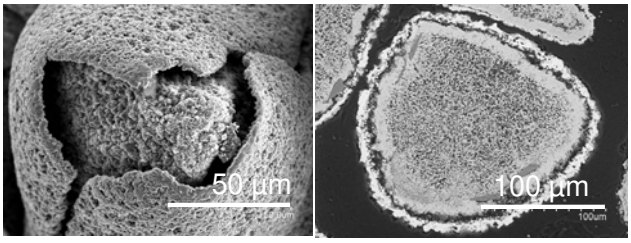

Figure 9: SEM micrograph of a particle and image of a cross section of a particle of activated ilmenite.

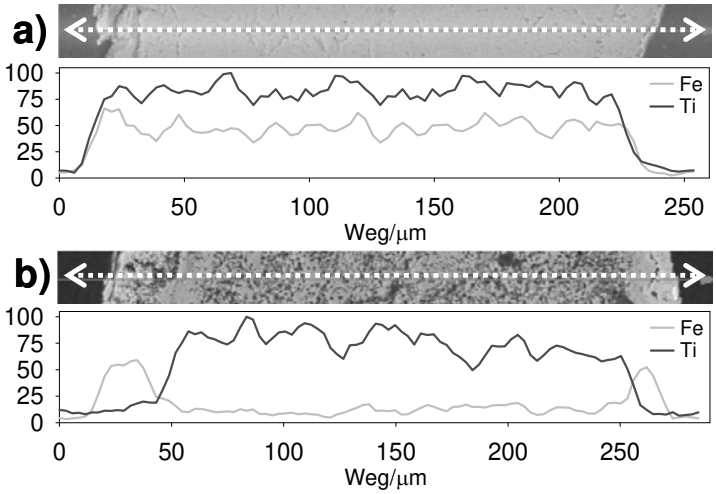

Figure 10. EDX line profiles of Fe and Ti in calcined (a) and activated (b) ilmenite particle.

Oxygen transport capacity, $R_{o,ilm}$. In addition to the OC reactivity, the oxygen transport capacity is a fundamental property of the OC since it determines the recirculation rate and solids inventory in the system, and therewith the suitability of ilmenite as oxygen carrier in CLC. The oxygen transport capacity of ilmenite can be obtained from equation (8) as the mass fraction of oxygen that can be used in the oxygen transfer. For CLC application, the oxygen transport capacity was defined as the oxygen that the oxygen carrier can supply to reach full conversion to CO_2 and H_2O at the thermodynamic equilibrium. Initially, equation (8) was used to obtain a value of R_o = 4.8% which was used to calculate the normalized conversions, $X_{N,r}$ and $X_{N,o}$. This value corresponded to the oxygen transport observed during TGA experiments using 15% H_2 + 20% H_2O, 15% CO + 20% CO_2 or 15% CH_4 + 20% H_2O in the reacting gases, see Figure 2. At these conditions, Fe_2TiO_5 reduces to $FeTiO_3$ and Fe_2TiO_4[28] and free Fe_2O_3 to FeO.[16] However, free Fe_2O_3 is only capable to fully convert CO and H_2 into CO_2 and H_2O when it is reduced to Fe_3O_4. Further reduction to FeO prevent full conversion of CO and H_2 towards CO_2 and H_2O because of thermodynamic limitations.[16] Thus, the oxygen transport capacity for ilmenite, $R_{o,ilm}$, must be obtained considering that in the reduced state Fe is present as $FeTiO_3$ or Fe_3O_4. Therefore, $R_{o,ilm}$ depends on the relative abundance of free Fe_2O_3 and iron titanates, which varies with the number of redox cycles.

To evaluate the fraction of Fe as Fe_2TiO_5 or Fe_2O_3 as a function of the number of redox cycles, different samples of calcined ilmenite were exposed at 10, 20, 30, 40, 50, 70, 85 and 100 redox cycles with 15 vol.% H_2, CO or CH_4 as fuel gas during the reduction period. The oxidation and reduction periods were 1 min. Particles subjected to different numbers of redox cycles had different activation degree and they were analyzed by XRD. Semi-quantitative percentages of Fe_2O_3 and Fe_2TiO_5 in each sample were obtained through normalization by means of a ratio between the intensity peaks of the main specie and a substance of reference. Figure 11 shows the mass fraction of Fe_2TiO_5 and Fe_2O_3 in the ilmenite particles as a function of the number of cycles when H_2 was used as reducing gas.

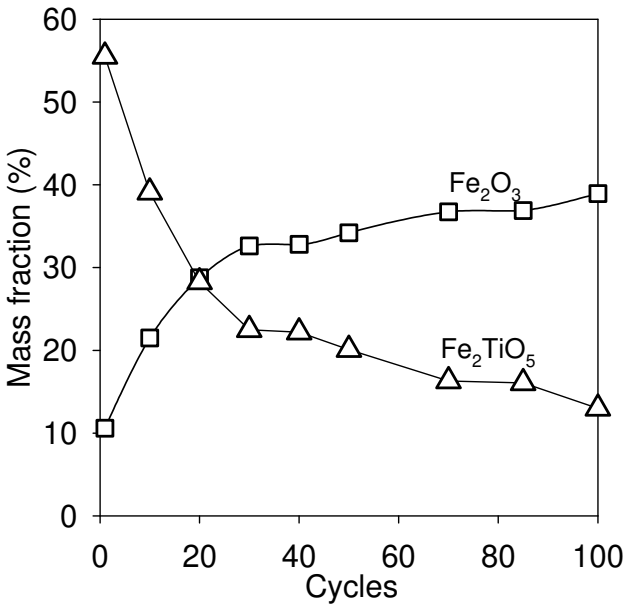

Figure 11. Mass fraction of Fe_2O_3 and Fe_2TiO_5 in ilmenite after 10, 20, 30, 40, 50, 70, 85 and 100 redox cycles. Oxidation and reduction periods were 1 min. Reducing gas used: 15% H_2 + 20% H_2O. Nitrogen to balance. T = 1173 K.

As the number of cycles increases, the fraction of free Fe_2O_3 rises at the expenses of Fe_2TiO_5. With these percentages the $R_{o,ilm}$ can be calculated, according to the formula:

$$R_{o,ilm} = R_{o,Fe_2O_3} x_{Fe_2O_3} + R_{o,Fe_2TiO_5} x_{Fe_2TiO_5} \quad (9)$$

R_{o,Fe_2O_3} is the oxygen transport capacity of Fe_2O_3 when converted to Fe_3O_4 (R_{o,Fe_2O_3} = 3.3%) and R_{o,Fe_2TiO_5} is the oxygen transport capacity of Fe_2TiO_5 when converted to $FeTiO_3$ (R_{o,Fe_2TiO_5} = 6.7%). $x_{Fe_2O_3}$ and $x_{Fe_2TiO_5}$ are the mass fractions of Fe_2O_3 and Fe_2TiO_5, respectively.

Figure 12(a) shows the evolution with the number of redox cycles of the oxygen transport capacity obtained from equation (9), $R_{o,ilm}$, for the different gases used. These values were confirmed by reduction of the different activated ilmenite samples in TGA using a H_2O/H_2 ratio of 50. At this ratio it is ensured that free Fe_2O_3 is unable to get reduced further than Fe_3O_4, while Fe_2TiO_5 is reduced to $FeTiO_3$ + Fe_2TiO_4. The mass variation so obtained gave similar values of $R_{o,ilm}$ than those obtained using equation (9). The initial $R_{o,ilm}$ value for calcined ilmenite was 4 wt.%. However, the fraction of free Fe_2O_3 increases with the number of cycles. As a consequence, the oxygen transport capacity decreases because free Fe_2O_3 reduction to Fe_3O_4 transfers less oxygen than reduction to Fe^{2+}. This decrease of $R_{o,ilm}$ is starker for the first cycles and after the activation period it decreases slight and continuously. The differences observed among the gases used were because of the different ilmenite conversion reached during the redox cycles, which affect to the activation process as it has been previously stated. After 100 redox cycles $R_{o,ilm}$ has a value of 2.1 wt.%, but still a stable value was not reached.

Evaluation of the feasibility of ilmenite as oxygen carrier. The use of a specific oxygen carrier has important implications for a CLC system.[40] The reduction and oxidation reactivity of solids determines the solids inventory in the fuel and air reactors, respectively, to reach full conversion of fuel gas. Moreover, the oxygen transport capacity is a fundamental property of the OC since it determines the recirculation rate and solids inventory in the system.

To facilitate a comparison of reactivity between different oxygen carriers a rate index is often used as a normalized rate at a fuel gas concentration of 15%.[36] The rate index, expressed in %/min is calculated as

$$Rate\,index = 100 \cdot 60 \cdot \left(\left| \frac{d\omega}{dt} \right| \right)_{norm} = 100 \cdot 60 \cdot R_{o,ilm} \left(\frac{dX_i}{dt} \right)_{norm} \quad (10)$$

The mass based conversion, ω, was defined as

$$\omega = \frac{m}{m_o} = 1 + R_{o,ilm} \left(X_o - 1 \right) = 1 - R_{o,ilm} X_r \quad (11)$$

Ilmenite conversion X_i of the oxidation or reduction reaction was obtained using equations (6) and (7) and considering that free Fe_2O_3 and Fe_2TiO_5 in ilmenite are reduced to Fe_3O_4 and $FeTiO_3$, respectively. Now the actual oxygen transport capacity, $R_{o,ilm}$, is used instead of the initial value R_o. The normalized reactivity is calculated as

$$\left(\frac{dX_i}{dt} \right)_{norm} = \frac{p_{ref}}{p_{TGA}} \left(\frac{dX_i}{dt} \right) \quad (12)$$

where p_{ref} is the reference partial pressure of the fuel gas, here equal to 0.15 atm, and p_{TGA} is the partial pressure of the fuel gas used in the TGA experiments. For the reduction reaction, the fuel gas concentration used in the TGA experiments were 15% in all cases (CH_4, CO and H_2). However, for the oxidation reaction, air was used as reacting gas. In this case, p_{TGA} = 0.21 atm and p_{ref} = 0.10 atn. The reactivity, (dX_i/dt), is here defined as the variation of conversion with time at conversion zero. For the reduction cases, this value is maintained roughly constant until conversion values as high as 60–80%, see Figures 3-6.

Figure 12(b) shows the variation of the reactivity of ilmenite with the number of cycles. During the activation period, which was previously determined to be 9 cycles with H_2, 20 cycles with CO and 30 cycles with CH_4, there is a considerable increase in the reaction rate. The slower reaction rate increase observed after this period was due to a concomitant effect of the variation of the oxygen transport capacity, $R_{o,ilm}$, on the conversion values. As previously has been shown, the oxygen transport capacity decreased with the cycle number. Therefore, the effect of ilmenite activation on the performance of a CLC system has a trade-off between the increase in reactivity and the decrease in oxygen transport capacity.

Figure 12(c) shows the rate index for every reacting gas as a function of the number of cycles. In this case, the reactivity is expressed as the rate of transference of oxygen by means of a mass fraction with respect the ilmenite mass. It is observed that the rate index increased during the activation period and eventually it reached a maximum and stable value that was kept constant during the cycles. This fact was expected from the normalized conversion curves showed in Figure 7, where the normalized conversion was calculated using a constant value of R_o = 4.8 wt.%.

The maximum value of the rate index was around 5.1 %/min for H_2, 1.6 %/min for CO, 3.1 %/min for CH_4 and 8.1 %/min for O_2. The rate index obtained for CH_4 is comparable to the rate index of 4.3 %/min obtained from TGA experiments for a synthetic Fe_2O_3/Al_2O_3 oxygen carrier.[40] A lower value of 2.8 %/min was obtained by Johansson[41] for the same oxygen carrier from FB experiments. This lower value could be due to gas transfer limitations between bubble and emulsion phases that affects the reactivity obtained in the FB. Also from FB experiments, Johansson[36,41] showed that the rate index for several synthetic iron-based carriers was in the range 0.5-4 %/min for CH_4 combustion, which is in line to the rate index showed for activated ilmenite. This fact agrees with the results showed by Leion et al.[29] where it was concluded that ilmenite reacts just as well as a synthetic $Fe_2O_3/MgAl_2O_4$ oxygen carrier. However, higher reactivities were found for the Fe_2O_3/Al_2O_3 oxygen carrier with H_2, CO and O_2 from TGA experiments.[16] The calculated rate index from results showed by Abad et al.[16,40] were 9 %/min for 15 vol.% CO, 21 %/min for 15 vol.% H_2, and 14 %/min for 10% O_2, which are considerably higher than the rate index showed by activated ilmenite. Nevertheless, it is necessary to remark that ilmenite is a natural mineral and a considerably cheaper material than a synthetic material.

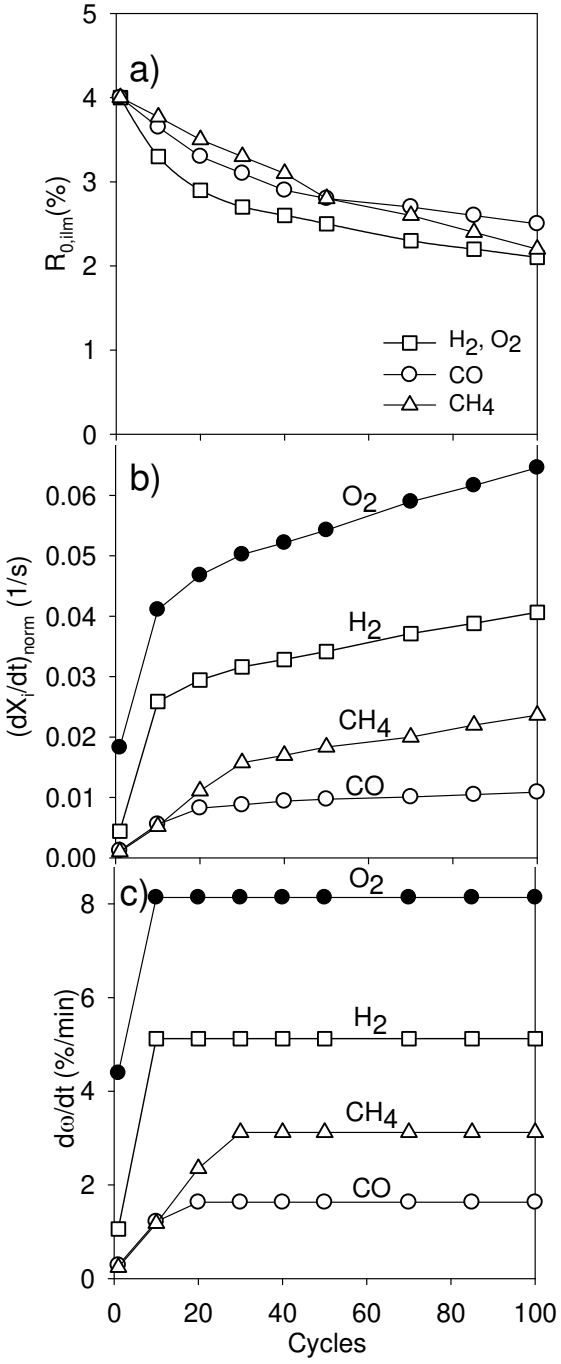

Figure 12. Variation of (a) the oxygen transport capacity, (b) the normalized reactivity, and (c) the rate index with the number of redox cycles. Oxidation and reduction periods were 1 min. Reacting gases: 15% H_2, 15% CO, 15% CH_4, and 10% O_2. Nitrogen to balance. T = 1173 K.

Applications to Design. The important parameters in the design of a CLC system are the recirculation rate of particles and the solids inventory. These parameters will be determined in this section for the use of ilmenite as oxygen carrier following the methodology showed by Abad et al.[40] The CLC concept is based on the circulating fluidized bed (CFB) configuration, and the circulation rate depends on the operating conditions and configuration of the riser. Abad et al.[40] took a circulation rate value of $\dot{m}_{OC}$ = 16 kg s^{-1} per MW_{th} as the maximum circulation rate feasible in a CLC plant without increased costs according to commercial experience on CFB systems. Thus, in a real CLC system the solids circulation may be fixed by the primary design of the AR, which acts as a riser to transport the solids to the FR. The recirculation rate between the air and fuel reactors must be high enough to transport oxygen necessary for the fuel combustion, and it determines the solid conversion variation in the reactors. For combustion of gaseous fuels, e.g. CH_4 or syngas, the solid conversion variation in the reactors is calculated from a mass balance as a function of the solids circulation rate per MW_{th} of fuel, $\dot{m}_{OC}$, as

$$\Delta X = \frac{2 d M_O}{R_{o,ilm} \Delta H_c^0} \frac{1}{\dot{m}_{OC}} \tag{13}$$

The solid conversion variation, ΔX, increases as the oxygen transport capacity, $R_{o,ilm}$, decreases, as can be seen in Figure 13(a). Using the value $\dot{m}_{OC}$ = 16 kg s^{-1} per MW_{th}, the solid conversion variation changes from ΔX = 0.09-0.12 when $R_{o,ilm}$ = 4.0 % to ΔX_i = 0.14-0.23 for the $R_{o,ilm}$ corresponding to particles after 100 redox cycles, depending on the fuel gas. For syngas combustion, the ΔX value should be between those values for H_2 and CO, and will depend on the syngas composition.

For combustion of solid fuels, e.g. coal, the solid conversion variation, ΔX, depends on the solids circulation rate and the solid fuel type. In a similar way to equation (13), ΔX can be calculated as

$$\Delta X_i = \frac{10^3 m_O}{R_{o,ilm} \mathrm{LHV}} \frac{1}{\dot{m}_{OC}} \tag{13}$$

with m_O the mass of oxygen required per kg of solid fuel to fully convert the solid fuel to CO_2 and H_2O, and LHV the lower heating value of the solid fuel. It is necessary to point out that m_O is the oxygen required for coal combustion, although the main reaction of coal particles in the fuel reactor is steam coal gasification. This is because the sum of reactions taking place in the fuel reactor, i.e. reactions (1-4), is the coal combustion. The steam fed into the fuel reactor does not supply oxygen for the coal combustion and only acts as a gasification agent.

In this work a typical composition for coal of 70% carbon, 5% hydrogen and 10% oxygen has been assumed, corresponding to a value of m_O = 2.2 kg O/kg coal. The LHV was assumed to be 25000 kJ/kg, and the solids circulation rate per MW_{th} of fuel equal to the value for gaseous fuels, i.e. $\dot{m}_{OC}$ = 16 kg s^{-1} per MW_{th}. The conversion variation, ΔX, so obtained is shown in Figure 13(a). In this case, it was assumed that the activation process follows the behavior showed by the reduction using H_2. It can be seen that the ΔX values are somewhat higher than the values obtained for gaseous fuels because the oxygen demand for coal is higher than this for CH_4, H_2 and CO per MW_{th} of fuel, which are 0.087, 0.08, 0.066, and 0.057 kg of oxygen per MJ for coal, CH_4, H_2 and CO, respectively. Moreover, ΔX also increases as the number of cycles increases because of the decrease of oxygen transport capacity. The low values obtained for ΔX indicate that ilmenite has enough oxygen transport capacity to be used as oxygen carrier in a CLC system, for gaseous and solid fuels.

The reactivity data obtained can be used to design the fuel (FR) and air (AR) reactors in a CLC system, i.e., to obtain the solids inventory necessary to fully convert the gas fuel. In a CLC process, it is desirable to minimize the amount of bed material in the reactors because this will reduce the size and investment cost of the system and less power will be needed by the fans that supply the reacting gases to the reactors.

For combustion of gaseous fuels, e.g. CH_4 or syngas, a simplified model has been used to get an initial estimation of the solids inventory and for comparison purposes among different oxygen carriers.[16,40] This model considers perfect mixing of solids, no restriction for the gas-solid contact, and

the solid reaction following the shrinking core model. In this case, the bed mass in the FR and AR per MW_{th} of fuel, m_{OC}, can be calculated as[16,40]

$$m_{OC} = \eta_c \frac{2dM_O}{\Delta H_c^0} \frac{3}{\Phi R_{o,ilm} \left(\frac{dX_i}{dt} \right)_{av}} = \eta_c \frac{2dM_O}{\Delta H_c^0} \frac{3}{\Phi \left(\left| \frac{d\omega}{dt} \right| \right)_{av}} \quad (15)$$

The average reactivities, $(dX_i/dt)_{av}$ and $(d\omega/dt)_{av}$, are obtained at the average gas concentration in the reactor. In line with other works,[36,41] an average gas concentration of 15% for fuel gas and 10% for oxygen is considered. Thus, the average reactivity corresponds to the normalized values previously showed. The parameter Φ was defined as the characteristic reactivity of the particles in the reactor.[40] This parameter involves the effect of both the residence time distribution of the particles in the reactor and the fact that particles entering to the reactor could have been not fully oxidized in the air reactor. Thus, higher average residence time or lower oxidation conversion in the air reactor, lower the average reactivity in the reactor is. With the assumption of perfect mixing of solid particles in the fuel and air reactors, the parameter Φ can be expressed as a function of the solid conversion at the inlet of the reactor, $X_{i,in}$, and the conversion variation in the reactor, ΔX

$$\Phi = 3\left[1 - X_{i,in}^{2/3} exp\left(-\frac{\left(1 - X_{i,in}^{1/3}\right)}{\Delta X}\Phi\right)\right] - \frac{6\Delta X}{\Phi}\left[1 - X_{i,in}^{1/3} exp\left(-\frac{\left(1 - X_{i,in}^{1/3}\right)}{\Delta X}\Phi\right)\right] + \frac{6\Delta X^2}{\Phi^2}\left[1 - exp\left(-\frac{\left(1 - X_{i,in}^{1/3}\right)}{\Delta X}\Phi\right)\right] \quad (16)$$

For the shrinking-core model in spherical grains, the value of characteristic reactivity, Φ, is limited between 3 and 0. The minimum solids inventory in every reactor is obtained considering that $\Phi = 3$, which is the case for $X_{i,in} = 0$ and $\Delta X \approx 0$. This condition could be reached when there were not limitations for solids circulation between FR and AR. However, as it has been previously discussed, a limitation for $\dot{m}_{OC} = 16$ kg s^{-1} per MW_{th} can be expected, which gives values of ΔX in the range 0.10-0.25, see Figure 13(a). The characteristic reactivity, Φ, decreases as ΔX increases, and the resulting solids inventory increases. This parameter can be obtained from equation (16) by an iterative calculation or more easily being estimated from Figure 7 in the work done by Abad et al.[40]

From results obtained in previous works,[40,42-44] the minimum solids inventory in a CLC system, considering the sum of solids in both AR and FR, is obtained for an intermediate situation between the full OC reduction in the FR and the full OC oxidation in the AR. To minimize the solids inventory, the inlet conversion to each reactor was found to be around the value $X_{i,in} = 0.5-\Delta X/2$. [40,42-44] For comparison purposes, the value for $X_{i,in}$ corresponding to every value of ΔX was used to obtain the solids inventory. Figure 13(b) shows the evolution of the solids inventory obtained from equation (15) with the number of cycles for H_2, CO and CH_4. It can be seen that the solids inventory decreases initially because the ilmenite reactivity increases during the activation process. After this period, the solids inventory slightly increases as $R_{o,ilm}$ decreases with the number of cycles. Indeed, the lower oxygen available in ilmenite as the number of cycle increases is the reason for both the increase in ΔX and in the solids inventory when the rate of oxygen transference, i.e. $d\omega/dt$, is constant, as this is the case. The solids inventory so obtained are about 85 kg/MW_{th} for H_2, 225 kg/MW_{th} for CO and 175 kg/MW_{th} for CH_4, after ilmenite activation. For a highly reactive synthethic Fe-based oxygen carrier similar solids inventory were obtained for CH_4,[40] whereas that for H_2 and CO the solids inventory are lower than for activated ilmenite, i.e. about 20 kg/MW_{th} for H_2 and 40 kg/MW_{th} for CO,[16,40] all of them referred to an average gas concentration of 15%. Nevertheless, the solids inventory needed for ilmenite takes acceptable values and in the same range as the values observed for synthetic OCs with proven suitability in a CLC process.[43]

For syngas, which is a gas mixture mainly composed by H_2, CO, H_2O and CO_2, the reactivity and the solids inventory have been found to be close to those showed for only H_2, with the H_2 concentration the sum of both H_2 and CO concentrations.[16,44] This fact can be due to the synergic effect of the water-gas shift reaction that produces more H_2 from the less reactive CO.[20,21]

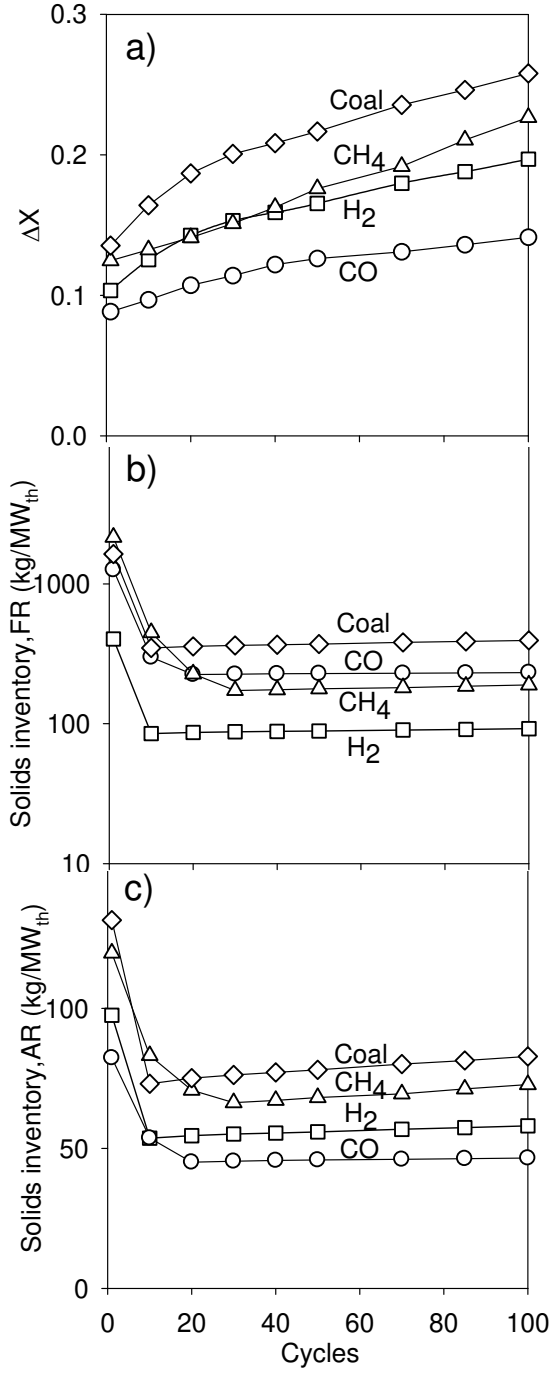

Figure 13. Calculated solid conversion variation between air and fuel reactors (a) and solid inventories, m_{OC}, in the fuel (b) and air (c) reactors for ilmenite reacted during several redox cycles. T = 1173 K. $\dot{m}_{OC}$ = 16 kg s^{-1} per MW_{th}. $X_{i,in}$ = 0.5-ΔX/2.

For solid fuels, the solids inventory can be calculated by analogy to equation (15) respecting equation (13) for gaseous fuels. Considering the oxygen demanded by the fuel calculated by equation (14), the solids inventory for solid fuels were obtained as

$$m_{OC} = \eta_c \frac{10^3 m_O}{\mathrm{LHV}} \frac{3}{\Phi R_{o,ilm} \left(\frac{dX_i}{dt}\right)_{av}} = \eta_c \frac{10^3 m_O}{\mathrm{LHV}} \frac{3}{\Phi \left(\left|\frac{d\omega}{dt}\right|\right)_{av}} \quad (17)$$

The reactivity parameters in this equation, i.e. $\left(\frac{dX_i}{dt}\right)_{av}$ or $\left(\left|\frac{d\omega}{dt}\right|\right)_{av}$, should be evaluated at an average gas concentration in the reactor. The main gases reacting with the oxygen carrier during operation with solid fuel are H_2 and CO proceeding from the char gasification and gases proceeding from the coal devolatilization that can be initially assumed to be CH_4. However, other important issues for volatiles compounds are the rate of mixing between oxygen carrier and coal particles and the injection point of coal inside the reactor,[30,31] being difficult at this stage to assign an average concentration for volatiles compounds. For comparison purposes, an initial estimation of the solids inventory was calculated only considering H_2 and CO proceeding from coal gasification. The average concentration of H_2 and CO in the reactor will depend on the dynamic of the reactions in the FR. It is likely that the concentration of these gases stabilizes at a value at which the generation rate from coal gasification is equal to the disappearance rate by reaction with the oxygen carrier. These concentration values can be as low as 2%, as has been found during CLC continuous operation using ilmenite as oxygen carrier[30,31] because the gasification reaction would be the limiting step in the process. Moreover, the H_2 and CO concentrations would be roughly constant in the whole reactor. Considering that the reactivity of a mixture of H_2 and CO is similar to the reactivity for H_2,[16,44] as it has been stated above, the average reactivity was calculated for H_2. The H_2 concentration was considered to be 5%, as the sum of H_2 and CO concentrations, and the average reactivity was calculated from equation (12) with p_{ref} = 0.05 atm H_2.

Figure 13(b) shows the solids inventory so obtained from equation (17). Similar to gaseous fuels, the initial solids inventory value is high because the reduction rate is rather low and ilmenite is not yet activated. The minimum solids inventory is obtained after the activation period, when the oxygen

transport capacity, $R_{o,ilm}$, has still high values. The solids inventory increases with the number of cycles because of the decrease in $R_{o,ilm}$. The solids inventory after ilmenite activation takes an average value about 350 kg/MW_{th}.

The solids inventory in the air reactor can be obtained from equations (15) and (17) for gaseous and solids fuels, respectively.[40] In this case, the average reactivity, i.e. $\left(\frac{dX_i}{dt}\right)_{av}$ or $\left(\left|\frac{d\omega}{dt}\right|\right)_{av}$, should be the corresponding to the oxidation reaction. As the oxygen demanded by each fuel (CH_4, H_2, CO or coal) is different per MW_{th} of fuel, the solids inventory per MW_{th} in the air reactor is also different for every fuel gas, even if the oxidation reactivity is the same in all cases. Therefore, a solids inventory in the air reactor can be calculated for each fuel gas, as it is shown in Figure 13(c). Lower values of the solids inventory are found for the air reactor than for the fuel reactor because of the higher ilmenite reactivity for the oxidation reaction with respect to the reduction reactions.

It must be remarked that all these values for solids inventory correspond to conditions where the resistance to the gas exchange between the bubble and emulsion phases are considered negligible. In real systems, if the resistance to the gas exchange between the bubble and emulsion phases is important, higher solids inventories would be necessary. Nevertheless, these values can be used for comparison purposes between different oxygen carriers and to give an easy and fast evaluation of the solids inventory in a CLC system. A FB model must be used to give a more accurate evaluation of the solids inventory needed in the FR.[45]

In any case, from results showed in this work, it can be concluded that ilmenite presents a competitive performance for its use in CLC against synthetic oxygen carriers when it is taken into account for the oxygen transport capacity, the moderated solids inventory and the low cost of the material. This last issue can be determinant for the selection of an oxygen carrier for solid fuels combustion in a CLC system.

CONCLUSIONS

The activation process of ilmenite through consecutives redox cycles has been analyzed. Ilmenite increases its reactivity with the number of cycles. For reducing and oxidizing periods of 30 minutes, it can be considered that from cycle 4 the reaction rate has already become maximum and stable, reaching complete conversion in every cycle. For reducing periods of 1 min the activation takes in about 9 cycles with H_2, 20 cycles with CO and 30 cycles with CH_4. The different activation behavior with different gases was attributed to the different reduction degree reached for each fuel gas in every cycle. A previous calcination of ilmenite has a positive effect on the activation process. After activation, the reactivity for H_2 and CO rises around 5 times, while for CH_4 this increase is about 15 times. Reduction and oxidation rates of activated ilmenite are relative high, with a conversion of 80% in less than 5 minutes. Reaction with H_2 is faster than with CO and CH_4.

Structural changes on the ilmenite particles after calcination and activation have been observed. The surface texture changes from a quite sharp-edged surface in fresh ilmenite to a granular shape in calcined samples. The granular shape was enhanced during the activation process. The porosity slightly increases during calcination. After activation the porosity of particles increases up to values of 35%. It was observed the appearance of cracks and an external shell in the particle, which is Fe enriched. All of them can explain the increase of ilmenite reactivity with the redox cycles.

As activation proceeds the reactivity increases, but the oxygen transport capacity of ilmenite, $R_{o,ilm}$, decreases due to the appearance of free Fe_2O_3 in the external shell. Thus, the-initial $R_{o,ilm}$ value is 4%, and it decreases until 2.1% after 100 redox cycles with hydrogen as fuel gas.

In comparison to other oxygen carriers and in particular to iron-based carriers, the $R_{o,ilm}$ and reactivity values showed for calcined and activated ilmenite have high enough values to transfer the required oxygen from air to fuel in a CLC system and to get acceptable values of minimum solids inventories in the system and good performance of ilmenite for a CLC purpose with solid fuels. A simplified method for the estimation of solids inventory in the air and fuel reactor was proposed for solid fuels. The solids inventory in the fuel reactor so obtained depended on the activation progress, decreasing from 1600

1 kg/MW_{th} to 350 kg/MW_{th} for coal during the activation period. These values can be used for
2 comparison purposes among oxygen carriers.
3
4 ACKNOWLEDGMENT
5 This work was partially supported by the European Commission, under the RFCS program (ECLAIR
6 Project, Contract RFCP-CT-2008-0008) and from Alstom Power Boilers. A. Cuadrat thanks CSIC for
7 the JAE Pre fellowship.
8
9

1 NOMENCLATURE

2 d = stoichiometric factor in the fuel combustion reaction with oxygen, mol O_2 per mol of fuel

3 ΔH_c^0 = standard combustion heat of the gas fuel, kJ mol^{-1}

4 m = instantaneous mass of the OC, kg

5 m_o = mass of fully oxidized OC, kg

6 m_r = mass of fully reduced OC at the reacting condition, kg

7 m_O = mass of oxygen required per kg of solid fuel to full convert the solid fuel, kg oxygen/kg coal

8 m_{OC} = solids inventory, kg/MW_{th}

9 $\dot{m}_{OC}$ = solids circulation rate per MW_{th} of fuel, kg s^{-1} per MW_{th}

10 M_O = molecular weight of oxygen, 16 g mol^{-1}

11 p_{ref} = reference partial pressure of the fuel gas, atm

12 p_{TGA} = partial pressure of the fuel gas used in the TGA experiments, atm

13 R_o = oxygen transport capacity for the normalized case

14 $R_{o,ilm}$ = actual oxygen transport capacity of ilmenite

15 R_{o,Fe_2O_3} = oxygen transport capacity of Fe_2O_3

16 R_{o,Fe_2TiO_5} = oxygen transport capacity of Fe_2TiO_5

17 t = time, s

18 T = temperature, K

$x_{Fe_2O_3}$ = mass fraction of Fe_2O_3

$x_{Fe_2TiO_5}$ = mass fraction of Fe_2TiO_5

X_i = ilmenite conversion for the reaction i

$X_{i,in}$ = solid conversion at the inlet of the reactor

$X_{N,i}$ = normalized conversion for the reaction i

ΔX = variation of the solids conversion

Greek symbols

η_c = combustion efficiency

ω = mass based conversion

Φ = characteristic reactivity in the reactor

Acronyms

AR = Air Reactor

CLC = Chemical Looping Combustion

FB = Fluidized Bed

FR = Fuel Reactor

LHV = Lower Heating Value of the solid fuel, kJ/kg

OC = Oxygen Carrier

Subscripts

av = average condition

i = oxidation (o) or reduction (r) reaction

ilm = ilmenite

norm = normalized gas concentration

1 REFERENCES

2 (1) *Climate Change 2007. Synthesis Report,* Contribution of Working Groups I, II and III to the
3 Fourth Assessment Report of the Intergovernmental Panel on Climate Change. Geneva, Switzerland,
4 **2007**, available in www.ipcc.ch.

5 (2) *International Energy Outlook 2008*, IEA. Washington. DC, U.S, **2008**.

6 (3) Eide, L.I.; Anheden, M.; Lyngfelt, A.; Abanades, C.; Younes, M.; Clodic, D. *Oil Gas Sci. Tech.*
7 **2005**, 60, 497–508.

8 (4) Kerr, H.R. *Capture and separation technologies gaps and priority research needs*; in: Thomas, D.,
9 Benson, S. (Eds.), Carbon Dioxide Capture for Storage in Deep Geologic Formations—Results from the
10 CO_2 Capture Project; Elsevier Ltd.: Oxford, UK, **2005**; vol. 1, chapter 38.

11 (5) Hossain, M.M.; de Lasa, H.I. *Chem. Eng. Sci.* **2008**, 63, 4433-4451.

12 (6) Lyngfelt, A.; Leckner, B.; Mattisson, T. *Chem. Eng. Sci.* **2001**, 56, 3101–3113.

13 (7) Ryu, H. J.; Jin, G. T.; Yi, C. K. *Demonstration of inherent CO_2 separation and no NOx emission*
14 *in a 50 kW chemical-looping combustor: Continuous reduction and oxidation experiment.* In
15 Proceedings of the Seventh International Conference of Greenhouse Gas Control Technologies; Wilson,
16 M., Morris, T., Gale, J., Thambibutu, K., Eds.; Elsevier Ltd.: Amsterdam, The Netherlands, **2005**; Vol.
17 2, pp 1907.

18 (8) Lyngfelt, A.; Thunman, H. *In Carbon Dioxide Capture for Storage in Deep Geologic Formations-*
19 *Results from the CO_2 Capture Project*; Thomas, D., Benson, S., Eds.; Elsevier Science: Amsterdam,
20 Netherlands, **2005**; vol. 1, Chapter 36.

21 (9) Linderholm, C.; Abad, A.; Mattisson, T.; Lyngfelt, A. *Int. J. Greenhouse Gas Control* **2008**, 2,
22 520–530.

(10) Linderholm, C.; Mattisson, T.; Lyngfelt, A. *Fuel* **2009**, 88, 2083-2096.

(11) Kolbitsch, P.; Pröll, T.; Bolhar-Nordenkampf, J.; Hofbauer, H. *Energy Procedia* **2009**, 1, 1465-1472.

(12) Adánez, J.; Gayán, P.; Celaya, J.; de Diego, L. F.; García-Labiano, F.; Abad, A. *Ind. Eng. Chem. Res.* **2006**, 45, 6075–6080.

(13) Jin, H.; Ishida, M. *Fuel* **2004**, 83, 2411-2417.

(14) Wolf, J.; Anheden, M.; Yan, J. *Performance Analysis of Combined Cycles with Chemical Looping Combustion for CO_2 Capture.* In International Pittsburg Coal Conference, Newcastle, New South Wales, Australia, Dec 3-7, **2001**.

(15) Mattisson, T.; García-Labiano, F.; Kronberger, B.; Lyngfelt, A.; Adánez, J.; Hofbauer, H. *Int. J. Greenhouse Gas Control* **2007**, 1, 158–169.

(16) Abad, A.; García-Labiano, F.; de Diego, LF.; Gayán, P.; Adánez, J. *Energy Fuels* **2007**, 21, 1843–1853.

(17) Johansson, E.; Mattisson, T.; Lyngfelt, A.; Thunman, H. *Chemical Engineering Research and Design*, **2006**, 84, 819–827.

(18)Abad, A.; Mattisson, T.; Lyngfelt, A.; Rydén, M. *Fuel,* **2006**, 85, 1174–1185.

(19) Abad, A.; Mattisson, T.; Lyngfelt, A.; M. Johansson. *Fuel*, **2007**, 86, 1021–1035.

(20) Dueso, C.; García-Labiano, F.; Adánez, J.; de Diego, L.F.; Gayán, P.; Abad, A. *Fuel* **2009**, 88, 2357-2364.

(21) Forero, C.R.; Gayán, P.; de Diego, L.F.; Abad, A.; García-Labiano, F.; Adánez, J. *Fuel Proces. Tech*. **2009**, 90, 1471-1479.

(22) Cao, Y.; Pan, W.-P. *Energy Fuels* **2006**, 20, 1836-1844.

(23) Dennis, J.S.; Scott, S.A., Hayhurst, A.N. (2006) *J. Energy Institute* **2006**, 79, 187-190.

(24) Cao, Y.; Casenas, B.; Pan, W.-P. *Energy Fuels* **2006**, 20, 1845-1854.

(25) Scott, S.A.; Dennis, J.S.; Hayhurst, A.N.; Brown, T. *AIChE J.* **2006**, 52, 3325-3328.

(26) Leion, H.; Mattisson, T.; Lyngfelt, A. *Fuel* **2007**, 86, 1947-1958.

(27) Zhao, H.; Liu, L.; Wang, B.; Xu, D.; Jiang, L.; Zheng, C. *Energy Fuels* **2008**, 22, 898-905.

(28) Leion, H.; Lyngfelt, A.; Johansson, M.; Jerndal, E.; Mattisson, T. *Chem. Eng. Res. Des.* **2008**, 86, 1017-1026.

(29) Leion, H.; Mattisson, T.; Lyngfelt, A. *Int. J. Greenhouse Gas Contro*, **2008**, 2, 180-193.

(30) Berguerand, N.; Lyngfelt, A. *Int. J. Greenhouse Gas Control* **2008**, 2, 169-179.

(31) Berguerand, N.; Lyngfelt, A. *Fuel* **2008**, 87, 2713-2726.

(32) Zhang, G.; Ostrovski, O. *Int. J. Min. Proc.* **2002**, 64, 201-218.

(33) Pröll, T.; Mayer, K.; Bolhàr-Nordenkampf, J.; Kolbitsch, P.; Mattisson, T.; Lyngfelt, A.; Hofbauer, H. *Energy Procedia* **2009**, 1, 27-34.

(34) Adánez, J.; De Diego, L.F.; García-Labiano, F.; Gayán, P.; Abad, A.; Palacios, J.M. *Energy Fuels* **2004**, 18, 371-377.

(35) Bhogeswara Rao, D.; Rigaud, M. *Oxidation of Metals* **1975**, 9, 99-116.

(36) Johansson, M.; Mattisson, T.; Lyngfelt, A. *Thermal Sci.* **2006**, 10, 93-107.

(37) Mattisson, T.; Lyngfelt, A.; Cho, P. *Fuel* **2001**, 80, 1953-1962.

(38) Rao, D.B.; Rigaud, M. *Oxidation of Metals* **1975**, 9, 99-116.

(39) Nell, J. *Heavy Minerals* **1999**, 137-145.

(40) Abad, A.; Adánez, J.; García-Labiano, F.; de Diego, L.F.; Gayán, P.; Celaya, J. *Chem. Eng. Sci*. **2007**, 62, 533-549.

(41) Johansson, M. *Screening of oxygen-carrier particles based on iron-, manganese-, copper- and nickel oxides for use in chemical-looping technologies.* Ph.D. Dissertation, Dept. Chemical and Biological Engineering, Environmental Inorganic Chemistry, Chalmers University of Technology, Göteborg, Sweden, 2007.

(42) Zafar, Q.; Abad, A.; Mattisson, T.; Gevert, B. *Energy Fuels* **2007**, 21, 610-618.

(43) Zafar, Q.; Abad, A.; Mattisson, T.; Gevert, B.; Strand, M. *Chem. Eng. Sci.* **2007**, 62, 6556-6567.

(44) García-Labiano, F.; de Diego, L.F.; Adánez, J.; Abad, A.; Gayán, P. *Ind. Eng. Chem. Res.* **2004,** 43, 8168–8177.

(45) Abad, A.; Adánez, J.; García-Labiano, F.; de Diego, L.F.; Gayán, P. *Combus. Flame* **2009**, doi:10.1016/j.combustflame.2009.10.010.